Organic LETTERS

Letter

pubs.acs.org/OrgLett

Solution-Processable n-Type Organic Semiconductors Based on Angular-Shaped 2-(12*H*-Dibenzofluoren-12-ylidene)malononitrilediimide

Debin Xia,[†] Tomasz Marszalek,[†] Mengmeng Li,[†] Xin Guo,[†] Martin Baumgarten,*[,†] Wojciech Pisula,[†,‡] and Klaus Müllen*[,†]

[†]Max Planck Institute for Polymer Research, Ackermannweg 10, 55128 Mainz, Germany

[‡]Department of Molecular Physics, Lodz University of Technology, Zeromskiego 116, 90-924 Lodz, Poland

Supporting Information

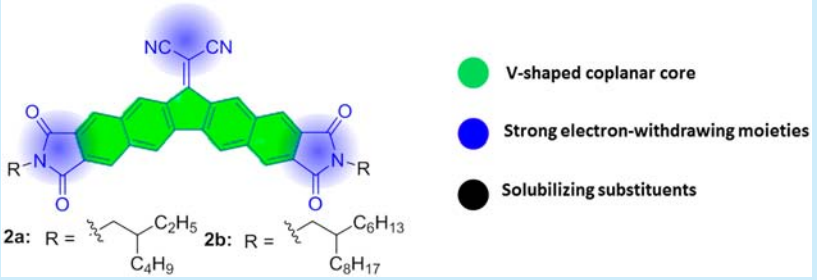

ABSTRACT: The angular-shaped n-type semiconductors 2-(12*H*-dibenzofluoren-12-ylidene)malononitrilediimide **2a** and **2b** were successfully designed, synthesized, and fully characterized by optical absorption and fluorescence, cyclic voltammetry, X-ray crystal structure analysis, XRD, and OFET device performance. The varying alkyl chain lengths of **2a** and **2b** caused different molecular orientations with respect to the substrate. Thus, **2a** presents an electron mobility of 0.01 $cm^2\ V^{-1}\ s^{-1}$, whereas **2b** resulted in poor device performance with a much lower electron mobility of $5 \times 10^{-4}\ cm^2\ V^{-1}\ s^{-1}$.

In recent years, organic field-effect transistors (OFETs) have attracted considerable attention.[1] Growing efforts have been devoted to n-type organic semiconductors,[2] but they largely lag behind those of the p-type counterpart. In order to obtain high performance materials for electron transport, there are three key factors: (1) suitable lowest unoccupied molecular orbital (LUMO) energy levels allowing efficient electron injection from metal electrodes that can be achieved by introduction of electron-withdrawing groups or atoms (benzothiadiazole, dicyanovinylenes, imides, fluorines, etc.) into known p-type molecules;[3] (2) coplanarity favoring strong $\pi-\pi$ intermolecular interaction and thus improving the charge carrier transport in the solid state;[4] and (3) an edge-on molecular orientation with respect to the substrate usually resulting in high-performance OFET, due to minimized grain boundaries and charge traps.[1d] As another factor, "shape" is rarely considered but is especially important, as it influences packing in the solid state. Almost all n-type organic semiconductors reported so far adopt linear arrangements.[1b,e,2b] Therefore, exploration of angular-shaped n-type molecules might expand the potential applications in OFETs.

Very recently, V-shaped molecules with extended π-conjugation have been revealed to be good candidates for p-type OFETs. For example, OFETs based on solution-crystallized dinaphthothiophene (DNT) (Figure 1) showed extremely high hole mobility as 9.5 $cm^2\ V^{-1}\ s^{-1}$ because of the suitable molecular arrangements in the solid states.[5] In another study, dinaphthocarbazole (DNC) (Figure 1) with seven fused rings presented good stability compared to the linear acene counterpart, arising from stabilization of the highest occupied molecular orbital (HOMO). Additionally, DNC exhibited a hole mobility of 0.055 $cm^2\ V^{-1}\ s^{-1}$ from solution-processed OFETs.[6] Considering both the high mobility of DNT and the

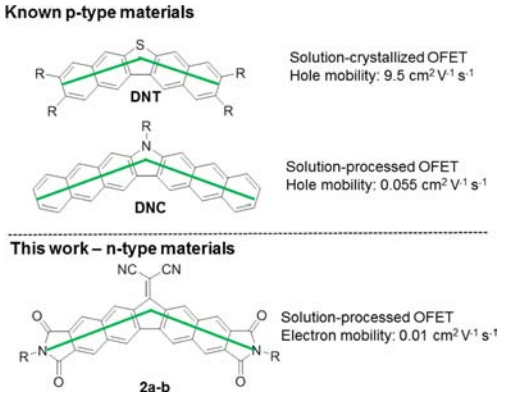

Figure 1. Structures of **DNT**, **DNC**, and **2a–b**.

Received: May 8, 2015
Published: June 9, 2015

DOI: 10.1021/acs.orglett.5b01343
Org. Lett. 2015, 17, 3074–3077

stability of the DNC of such V-shaped molecules, electron-withdrawing groups at the end points of the V-shaped coplanar core have been combined in the current design. This also enables the details of packing of these molecules between each other and with respect to the surface in comparison to linear fused acceptors to be studied.

Based on such a molecular design, 2-(12*H*-dibenzofluoren-12-ylidene)malononitrilediimides (**2a–b**, Figure 1) are expected to be good candidates as solution-processable n-type materials according to the following considerations: (1) the electron-withdrawing dicarboximides and dicyanovinylene units will dramatically lower the LUMO energy level for effective electron injection; (2) alkyl chains can be easily attached at the nitrogen atoms of the end-capped dicarboximides to induce solubility and formation of ordered thin films; and (3) the rigid and planar conjugated framework facilitates efficient intermolecular charge-transfer interaction. Herein, we report the synthesis, characterizations, physical properties, thermal behavior, and semiconducting characteristics.

2,3,6,7-Tetramethyl-9*H*-fluoren-9-one (**4**) is the key building block, as extension of π-conjugation can be achieved by the functionalization of tetramethyl and carbonyl groups of **4**. Compound **4** was achieved in 75% yield through Pd-catalyzed dehydrogenative cyclization (Scheme 1).[7] Radical bromination

Scheme 1. Synthesis of 1a–b and 2a–b

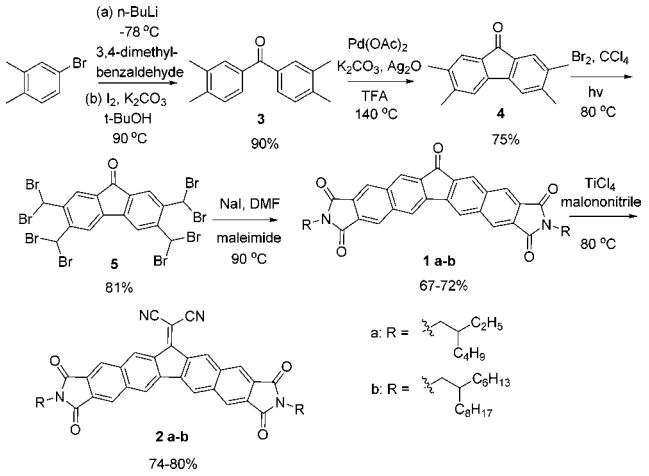

was done with bromine in CCl_4 upon irradiation with a 250 W halogen lamp, which afforded 2,3,6,7-tetrakis(dibromomethyl)-9*H*-fluoren-9-one **5** as a yellow solid in 81% yield. After treatment of fluorenone **5** with NaI in DMF, a Diels–Alder cycloaddition with maleimides containing different alkyl chains afforded **1a–b** in 67–72% yield. Finally, the target products **2a–b** were obtained in 74–80% yield by Knoevenagel condensation of **1a–b** with the Lehnert reagent[8] ($TiCl_4$, malononitrile, pyridine). The chemical structures of all new compounds were fully supported by standard spectroscopic characterizations and high resolution mass spectrometry (Supporting Information).

The UV–vis absorption and photoluminescence spectra of **1a–b** and **2a–b** were recorded in dichloromethane (DCM) solution (Figure 2A and Table S1). Compounds **1a** (**2a**) and **1b** (**2b**) displayed almost the same substructures in the absorption spectra and identical emission wavelengths because the alkyl chains do not influence the electronic properties in dilute solution.[9] The significant red shift of both the absorption

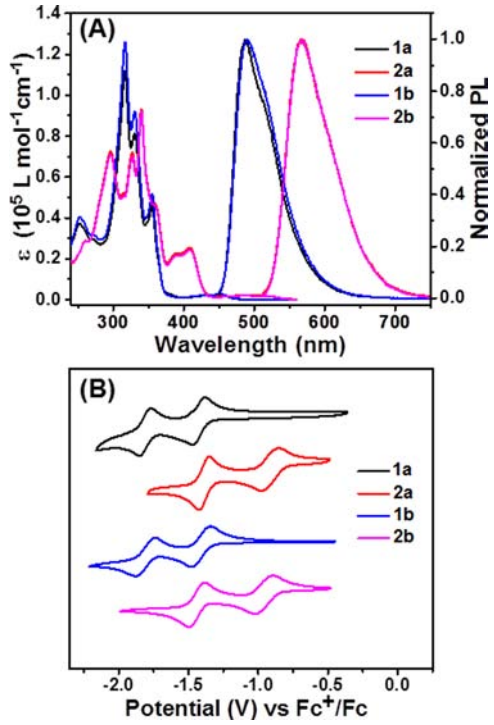

Figure 2. (A) UV–vis absorption spectra and fluorescence spectra of **1a–b** and **2a–b** in dichloromethane. (B) Cyclic voltammetric profile of **1a–b** and **2a–b** in dichloromethane with 0.1 M Bu_4NPF_6 as supporting electrolyte. Potentials are reported versus the Fc^+/Fc redox couple as an external standard, scan rate = 100 mV/s.

and emission spectra of **2** in comparison with **1** can be explained by the stronger electron-withdrawing malononitrile group, which decreases the LUMO more than the HOMO energies.[10] The optical gaps estimated from the onset of the absorption spectra are 2.60 and 2.25 eV for **1** and **2**, respectively (Table S1).

The redox properties of **1a–b** and **2a–b** were studied using cyclic voltammetry. Cyclic voltammograms of all compounds in DCM exhibited two reduction waves, with the $E_{1/2}$ potential around −1.39 V for **1** and −0.94 V for **2**, but no oxidation waves in the potential range available. The LUMO energies of **1** and **2** estimated through the equation $E_{LUMO} = -[E_{red1/2} - E_{(Fc^+/Fc)} + 4.8]$ eV were around −3.41 and −3.86 eV, respectively. The deeper LUMO level of **2** can be attributed to the stronger electron-withdrawing character of the dicyanovinylene group compared to that of the carbonyl moiety. The low-lying LUMO of **2** indicates that they could be well suited as n-type semiconductors with efficient electron injection.

Thermogravimetric analysis (TGA) revealed that **1a**, **1b**, **2a**, and **2b** exhibit good thermal stability, with a 5 wt % loss occurring at 442, 411, 441, and 404 °C, respectively (Figure S1). Differential scanning calorimetry (DSC) traces for **1a**, **1b**, **2a**, and **2b** showed melting points at 359, 235, 359, and 266 °C, respectively (Figure S2).

A single crystal of **2b** was grown by slow evaporation of DCM. The crystal structure determined by X-ray diffraction is presented in Figure 3. The dicyanomethylene moiety is slightly twisted with respect to the backbone of the core, which can be caused by the close proximity of the cyano groups and the hydrogen atoms. The crystal structure of **2b** involves face-to-face stacked dimers, which interact with each other in a one-

DOI: 10.1021/acs.orglett.5b01343
Org. Lett. 2015, 17, 3074–3077

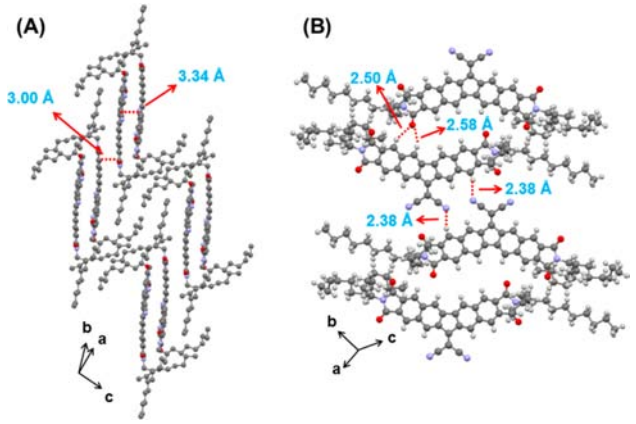

Figure 3. Crystal packing of **2b**. (A) Face-to-face $\pi-\pi$ stacking with an interplanar distance of 3.34 Å. (B) =O···H− and ≡N···H− hydrogen bonding between stacks.

dimensional, slipped-stack arrangement as shown in Figure 3A. Furthermore, =O···H− (2.50 and 2.58 Å) and ≡N···H− (2.38 Å) hydrogen bonds are an additional driving force contributing to the assembly of **2b**. This crystal arrangement is probably due to strong dipole−dipole interactions among the imide and cyano groups.

To understand the influence of the alkyl substitution of the V-shaped core on the surface self-organization of **2a** and **2b**, X-ray diffraction (XRD) of both polycrystalline samples was performed. Zone-casting, a solution processing method, was utilized for the film deposition. This technique has been reported to yield homogeneous and well-ordered polycrystalline films for various π-conjugated systems.[11] Figure S3 presents XRD diffractograms obtained for zone-cast **2a** and **2b**. The interlayer distance of 2.60 nm for **2a** is determined from the main reflection (100 according to the Miller's index) observed at q_z = 0.24 Å^{-1} (Figure S3A). Higher order reflections (up to eighth) imply long-range organization of the molecules in the out-of-plane direction of the film. This interlayer distance is in agreement with the theoretical molecule length of 2.65 nm calculated by Cerius^2.[12] This suggests that the long axis of the V-shaped molecule is arranged perpendicular to the silicon dioxide surface (Figure S4C). In this edge-on organization the π-stacking direction is oriented parallel to the surface which is beneficial for the charge carrier transport in field-effect transistors.

For **2b** the main reflection (100 according to Miller's index, Figure S3B) corresponds to a *d*-spacing of 2.00 nm which is in agreement with the *c* parameter of the triclinic unit cell obtained for the single crystal (Figure 3). It can be therefore concluded that the *c* axis is arranged in the out-of plane direction. In that case, **2b** is organized in face-to-face stacked dimers which are tilted with respect to the surface.

Indirect evidence for the tilting of **2b** is provided by polarized optical microscopy (POM) performed for the zone-cast layers (Figure S4). All polycrystalline layers exhibit birefringence between cross-polarizers. In the case of **2a**, the POM image remains dark when the crystal optical axis (or zone-casting direction) is arranged parallel to one of the polarizers (0° and 90°). Maximum birefringence is observed for the angle of 45°. In contrast, **2b** shows no light transmission for the angle of 45° indicating that axis *b* of the crystal is almost aligned parallel to the zone-casting direction (Figure S5). In such a crystal arrangement, the axis of the molecules is oriented around 45° toward the alignment direction resulting in a reverse extinction under POM compared to **2a**.

The charge carrier transport of **2a** and **2b** was investigated by fabricating OFET devices in the bottom-gate bottom-contact configuration. Before drop-casting from 2 mg/mL chloroform solution, the silicon wafer with 300 nm thick thermally grown SiO_2 was functionalized by hexamethyldisilazane (HMDS) to minimize interfacial trapping sites. Au was evaporated as the source and drain electrodes. The drop-cast films were annealed at 120 °C for 30 min to remove the residual solvent before OFET measurement. Figure 4 shows the transfer and output characteristics of **2a** and **2b**, respectively.

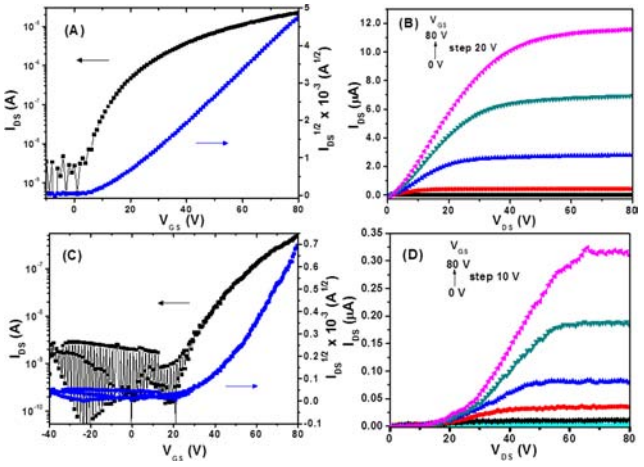

Figure 4. Transfer and output characteristics of OFET devices fabricated by drop casting of **2a** (A, B) and **2b** (C, D). For B and D, V_{DS} = 80 V is applied.

In the positive drain mode of both compounds, the drain current (I_{DS}) first exhibits linear behavior with increasing gate voltage (V_{GS}) and then becomes saturated (Figure 4 A and C). This transistor behavior is characteristic for an electron transporting semiconductor which can be attributed to the introduction of strong electron-withdrawing moieties. The maximum saturated electron mobility of **2a** is 0.01 cm^2 V^{-1} s^{-1} and the on/off ratio is around 10^4. The threshold voltage of 12 V is low compared to **2b** where the threshold voltage is increased to 35 V. Such high contact resistance for **2b** can only be explained with the molecular organization in the drop-cast film, also caused by disorder of the molecules close to the metal semiconductor interface. In comparison to **2a**, **2b** shows a relatively poor electron transport, with a maximum mobility of 5×10^{-4} cm^2 V^{-1} s^{-1} and an on/off ratio of 10^3. Zone-casting only slightly improved the device performance of **2b** yielding charge carrier mobilities of 1×10^{-3} cm^2 V^{-1} s^{-1}. The lower performance of drop-cast **2b** in comparison to **2a** is ascribed to the face-to-face organization of **2b** and molecular tilting induced by longer alkyl chains. Such organization of the molecules causes the π-stacking interaction to not be in-plane with the substrate.

In summary, two novel angular n-type molecules **2a** and **2b** have been successfully synthesized based on the 2,3,6,7-tetramethyl-9*H*-fluoren-9-one intermediate. While their electronic properties in diluted media are identical as proven by cyclic voltammetry and optical spectra with a low lying LUMO of −3.86 eV, the length of the alkyl chain plays a pivotal role in the molecular orientation relative to the surface. For **2a**, the

DOI: 10.1021/acs.orglett.5b01343
Org. Lett. 2015, 17, 3074−3077

molecules adopt an edge-on orientation with an OFET electron mobility of 0.01 $cm^2 V^{-1} s^{-1}$, while **2b** with longer branched chains is tilted with respect to the substrate, thereby resulting in poor device performance.

■ ASSOCIATED CONTENT

Supporting Information

Experimental details, synthesis, characterization, and theoretical studies. The Supporting Information is available free of charge on the ACS Publications website at DOI: 10.1021/acs.orglett.5b01343.

■ AUTHOR INFORMATION

Corresponding Authors

*E-mail: baumgart@mpip-mainz.mpg.de.
*E-mail: muellen@mpip-mainz.mpg.de.

Notes

The authors declare no competing financial interest.

■ ACKNOWLEDGMENTS

This work was financially supported by the Transregio TR49 and ERC-Adv.-Grant 267160 (NANOGRAPH). We acknowledge Dr. Dieter Schollmeyer at Johannes Gutenberg-University for crystal analysis.

■ REFERENCES

(1) (a) Guo, X.; Baumgarten, M.; Müllen, K. *Prog. Polym. Sci.* **2013**, *38*, 1832. (b) Mei, J.; Diao, Y.; Appleton, A. L.; Fang, L.; Bao, Z. *J. Am. Chem. Soc.* **2013**, *135*, 6724. (c) Di, C. A.; Zhang, F.; Zhu, D. *Adv. Mater.* **2013**, *25*, 313. (d) Wang, C. L.; Dong, H. L.; Hu, W. P.; Liu, Y. Q.; Zhu, D. B. *Chem. Rev.* **2012**, *112*, 2208. (e) Jiang, W.; Li, Y.; Wang, Z. *Chem. Soc. Rev.* **2013**, *42*, 6113.

(2) (a) Li, Y. N.; Sonar, P.; Murphy, L.; Hong, W. *Energy Environ. Sci.* **2013**, *6*, 1684. (b) Liu, Z.; Zhang, G.; Cai, Z.; Chen, X.; Luo, H.; Li, Y.; Wang, J.; Zhang, D. *Adv. Mater.* **2014**, *26*, 6965. (c) Durso, M.; Gentili, D.; Bettini, C.; Zanelli, A.; Cavallini, M.; De Angelis, F.; Grazia Lobello, M.; Biondo, V.; Muccini, M.; Capelli, R.; Melucci, M. *Chem. Commun.* **2013**, *49*, 4298. (d) Yanai, N.; Mori, T.; Shinamura, S.; Osaka, I.; Takimiya, K. *Org. Lett.* **2014**, *16*, 240. (e) Mori, T.; Yanai, N.; Osaka, I.; Takimiya, K. *Org. Lett.* **2014**, *16*, 1334.

(3) (a) Wu, Q.; Ren, S.; Wang, M.; Qiao, X.; Li, H.; Gao, X.; Yang, X.; Zhu, D. *Adv. Funct. Mater.* **2013**, *23*, 2277. (b) Li, H.; Kim, F. S.; Ren, G.; Hollenbeck, E. C.; Subramaniyan, S.; Jenekhe, S. A. *Angew. Chem., Int. Ed.* **2013**, *52*, 5513. (c) Shi, X.; Chang, J.; Chi, C. *Chem. Commun.* **2013**, *49*, 7135. (d) Ie, Y.; Ueta, M.; Nitani, M.; Tohnai, N.; Miyata, M.; Tada, H.; Aso, Y. *Chem. Mater.* **2012**, *24*, 3285. (e) Usta, H.; Kim, C.; Wang, Z.; Lu, S.; Huang, H.; Facchetti, A.; Marks, T. J. *J. Mater. Chem.* **2012**, *22*, 4459. (f) Guo, X.; Puniredd, S. R.; Baumgarten, M.; Pisula, W.; Müllen, K. *Adv. Mater.* **2013**, *25*, 5467. (g) Kono, T.; Kumaki, D.; Nishida, J.-i.; Tokito, S.; Yamashita, Y. *Chem. Commun.* **2010**, *46*, 3265.

(4) (a) Tian, H.; Deng, Y.; Pan, F.; Huang, L.; Yan, D.; Geng, Y.; Wang, F. *J. Mater. Chem.* **2010**, *20*, 7998. (b) Gao, P.; Beckmann, D.; Tsao, H. N.; Feng, X.; Enkelmann, V.; Baumgarten, M.; Pisula, W.; Müllen, K. *Adv. Mater.* **2009**, *21*, 213. (c) Liang, Z.; Tang, Q.; Mao, R.; Liu, D.; Xu, J.; Miao, Q. *Adv. Mater.* **2011**, *23*, 5514.

(5) Okamoto, T.; Mitsui, C.; Yamagishi, M.; Nakahara, K.; Soeda, J.; Hirose, Y.; Miwa, K.; Sato, H.; Yamano, A.; Matsushita, T.; Uemura, T.; Takeya, J. *Adv. Mater.* **2013**, *25*, 6392.

(6) Pho, T. V.; Yuen, J. D.; Kurzman, J. A.; Smith, B. G.; Miao, M.; Walker, W. T.; Seshadri, R.; Wudl, F. *J. Am. Chem. Soc.* **2012**, *134*, 18185.

(7) Li, H.; Zhu, R.-Y.; Shi, W.-J.; He, K.-H.; Shi, Z.-J. *Org. Lett.* **2012**, *14*, 4850.

(8) (a) Lehnert, W. *Tetrahedron Lett.* **1970**, *11*, 4723. (b) Lehnert, W. *Synthesis* **1974**, *1974*, 667.

(9) Yin, J.; Qu, H.; Zhang, K.; Luo, J.; Zhang, X.; Chi, C.; Wu, J. *Org. Lett.* **2009**, *11*, 3028.

(10) (a) Kozaki, M.; Yonezawa, Y.; Okada, K. *Org. Lett.* **2002**, *4*, 4535. (b) Usta, H.; Facchetti, A.; Marks, T. J. *Org. Lett.* **2008**, *10*, 1385. (c) Usta, H.; Facchetti, A.; Marks, T. J. *J. Am. Chem. Soc.* **2008**, *130*, 8580. (d) Jacques, E.; Romain, M.; Yassin, A.; Bebiche, S.; Harnois, M.; Mohammed-Brahim, T.; Rault-Berthelot, J.; Poriel, C. *J. Mater. Chem. C* **2014**, *2*, 3292.

(11) (a) Pisula, W.; Menon, A.; Stepputat, M.; Lieberwirth, I.; Kolb, U.; Tracz, A.; Sirringhaus, H.; Pakula, T.; Müllen, K. *Adv. Mater.* **2005**, *17*, 684. (b) Marszalek, T.; Nosal, A.; Pfattner, R.; Jung, J.; Kotarba, S.; Mas-Torrent, M.; Krause, B.; Veciana, J.; Gazicki-Lipman, M.; Crickert, C.; Schmidt, G.; Rovira, C.; Ulanski, J. *Org. Electron.* **2012**, *13*, 121.

(12) *Cerius 2 calculation*; Accelrys, Inc.: San Diego, CA, 1998.

DOI: 10.1021/acs.orglett.5b01343
Org. Lett. 2015, 17, 3074−3077